Available online at www.sciencedirect.com
ScienceDirect
Journal of the European Ceramic Society 29 (2009) 3401–3408
www.elsevier.com/locate/jeurceramsoc

# Reactive hot pressing of zirconium diboride

Adam L. Chamberlain [1], William G. Fahrenholtz *, Gregory E. Hilmas

*Department of Materials Science and Engineering, Missouri University of Science and Technology, 222 McNutt Hall, Rolla, MO 65409, United States*

Received 8 February 2009; received in revised form 29 May 2009; accepted 7 July 2009
Available online 3 August 2009

**Abstract**

The reaction of zirconium and boron was investigated as a potential route to form dense monolithic zirconium diboride ($ZrB_2$) ceramics. Attrition milling of the precursors produced nanosized (less than 100 nm) zirconium metal particles that reacted with boron to form $ZrB_2$ with an average particle size of less than 100 nm at temperatures as low as 600 °C. Scanning electron microscopy of $ZrB_2$ compacts heated to 1450 °C and 1650 °C showed average particle sizes of 0.6 μm and 1.0 μm, respectively, suggesting that the fine particle size was maintained during densification. Ceramics with a relative density of ~99% were produced by hot pressing at 2100 °C. Dense $ZrB_2$ produced by the reactive hot pressing process had mechanical properties that were comparable to ceramics produced by conventional processes. The four-point flexure strength of $ZrB_2$ produced in this study was 434 MPa.


*Keywords:* Borides; Reactive hot pressing; Strength

## 1. Introduction

Zirconium diboride ($ZrB_2$) is a transition metal boride that crystallizes into a hexagonal crystal structure of the $AlB_2$ type. This crystal structure consists of alternating layers of hexagonally closed packed metal atoms (M) and graphite-like boron (B) stacked in a MBMBMB sequence.[1] This structure results in strong covalent bonding between boron–boron and metal–boron atoms, while the close packed metal layers exhibit characteristics consistent with metallic bonding.[2,3] The combination of covalent and metallic bonding gives $ZrB_2$ an unusual combination of properties. The strong covalent bonding leads to a high melting temperature (3250 °C), high hardness (23 GPa), and high strength (~500 MPa).[4,5] The metallic bonding leads to low electrical resistivity ($10^{-5}$ Ω cm) and high thermal conductivity (~60 W/m K).[6,7] Because of this unusual combination of properties, $ZrB_2$ has been proposed for use in various high temperature structural applications.[8] The oxidation and thermal shock resistance of $ZrB_2$ also make it a candidate for thermal protection systems on future hypersonic flight vehicles.[9,10]

Processing of high melting temperature diborides such as $ZrB_2$, $HfB_2$, and $TiB_2$ has traditionally focused on using commercially available powders with the addition of various metallic and ceramic additives as sintering aids. Metallic additives (Fe, Ni, and Co) have been used to promote liquid phase formation that enhances densification by facilitating particle rearrangement and mass transport.[11] However, the addition of low melting temperature additives results in complete loss of strength by 1200 °C,[12] therefore, limiting their use in high temperature applications.

Ceramic additions that include silicon carbide, silicon nitride, boron carbide, metal silicides, and oxides have also been used to improve the densification of $ZrB_2$.[13–15] These additives enhance the densification of $ZrB_2$ ceramics between 1700 °C and 1900 °C. Densification of $ZrB_2$ at these moderate temperatures can result in fine grain microstructures (2–3 μm) that can exhibit strengths in excess of 1000 MPa.[5] However, the addition of ceramic additives can also significantly decrease the maximum operating temperature due to the formation of eutectic liquids. The most common additive to $ZrB_2$ is silicon carbide (SiC). The $ZrB_2$–SiC eutectic temperature is 2270 °C, which limits the use of these ceramics to temperatures below this value.

For $ZrB_2$ ceramics to operate at the highest possible temperatures, the use of ceramic or metallic additives must be minimized. Densification of $ZrB_2$ without sintering aids is difficult due

* Corresponding author. Tel.: +1 573 341 6343; fax: +1 573 341 6934.
*E-mail address:* billf@mst.edu (W.G. Fahrenholtz).
[1] Present address: Rolls-Royce, Inc., Indianapolis, IN, United States.

0955-2219/$ – see front matter © 2009 Elsevier Ltd. All rights reserved.
doi:10.1016/j.jeurceramsoc.2009.07.006

to its low intrinsic sinterability, which is a result of its strong covalent bonding as well as low volume and grain boundary diffusivities.[16] Improvements in the densification of high purity $ZrB_2$ require processing methods that can increase the driving force for densification by means other than additives.

Densification of $ZrB_2$ can be enhanced using reactive forming methods. The strongly exothermic reaction ($\Delta H^o_{rxn} = -323$ kJ) and the resulting high adiabatic temperature (3250 K) associated with the formation of $ZrB_2$ from Zr and B means that self-propagating high temperature synthesis (SHS) can be used to form this diboride.[17] $ZrB_2$ powders formed using SHS have exhibited increased sinterability, which has been attributed to the presence of lattice defects. These defects were attributed the rapid heating and cooling rates (~200,000 K/min) associated with SHS.[18] However, rapid heating rates can also result in incomplete reaction, the formation of non-equilibrium phases, the formation of stable oxides, or the retention of large amounts of porosity (>50%).[19] Densification of materials formed by SHS typically requires further powder processing and additional heat treatments.[20]

Like SHS, reactive hot pressing (RHP) is another method that relies on thermodynamically favorable reactions to form intermetallics, non-oxide ceramics, and metals.[21–23] Unlike SHS, RHP relies on a controlled (i.e., non-self-propagating) reaction in which the products are formed relatively slowly by a solid-state diffusion-controlled process. The use of controlled reactions ensures that the reactants are completely converted to the products. In addition, the combination of controlled reaction and the simultaneous application of pressure may produce dense specimens in a combined *in situ* synthesis and densification process, thereby eliminating the need for further powder processing after the reaction is complete.

Several groups have produced diboride based ceramics using RHP.[21,24,25] Some reports have indicated that dense $ZrB_2$ ceramics can be produced at temperatures that are 200–300 °C lower than conventional processing.[24–26] This reduction in processing temperature may be related to the minimization of oxide impurities ($B_2O_3$ and $ZrO_2$) that are thought to promote coarsening and inhibit densification of the boride ceramics. The use of base metal precursors also provides the opportunity to utilize nanoscale (<100 nm) precursors that can be used to produce ceramics with sub-micron grain sizes. The use of high energy milling to reduce the size of the metallic precursors may also result in the development of large defect concentrations in the precursors, which, in turn, may enhance densification of the resulting ceramics.[25,27]

This paper focuses on the reaction sequence between elemental Zr and B and the effect of powder processing on the reactive hot pressing of $ZrB_2$. The densification behavior, microstructure, and properties of the resulting $ZrB_2$ ceramics are also discussed.

## 2. Experimental procedure

### 2.1. Powder processing

The primary precursors for this study were Zr powder (00418, Alfa Aesar, Ward Hill, MA) and B powder (SB99, Reade Materials, Reno, NV). The Zr powder had a purity of 99% (metals basis, excluding Hf), a reported particle size of −325 mesh, and a surface area of 0.4 $m^2$/g. The B powder was amorphous with a reported purity of 99% (metals basis), an average particle size of 100 nm, and a surface area of 35 $m^2$/g. Powder batches containing 80.7 wt.% Zr and 19.3 wt.% B were attrition milled (Model HD-01, Union Process, Akron, OH) in hexane at 600 rpm for 240 min using a polymer coated bucket and tungsten carbide spindle and media. Milling reduced the particle size of the Zr metal and promoted homogenous mixing. To minimize segregation of Zr and B during drying, the hexane was removed using rotary evaporation (Rotavapor R-124, Bucchi, Flawil, Germany) at a temperature of 70 °C, vacuum of 300 mm Hg, and a rotation speed of 90 rpm.

During the attrition milling process, powder samples (~2 g) were removed after 20 min, 60 min, 90 min, 120 min, and 150 min of milling. Scanning electron microscopy (SEM; S-570, Hitachi, Tokyo, Japan) was performed to characterize the evolution of particle size and powder morphology as a function of time. X-ray diffraction (XRD; XDS 2000, Scintag, Cupertino, CA) analysis was used to determine the phases present in milled powders. Particle size calculations were performed on Zr–B powder mixtures using the Scherrer formula (Eq. (1))[28]:

$$t = \frac{0.9\lambda}{\beta \cos\theta} \quad (1)$$

where $t$ = crystallite size (Å), $\lambda$ = X-ray wavelength (1.5405 Å), and $\beta$ = full width at half maximum (rad).

Differential thermal analysis (TGA/DTA, Netzsch, Exton, PA) was performed on powder mixtures to determine how the reaction rates and onset temperature changed with milling time. Analysis was performed on powder samples up to 1500 °C using a heating rate of 10 °C/min in flowing argon.

### 2.2. Reactive hot pressing

Milled powders were uniaxially hot pressed (HP-3060, Thermal Technology, Santa Rosa, CA) in a boron nitride coated graphite die. Specimens were heated under vacuum (~150 mtorr) up to 1650 °C and then the hot press was backfilled with argon. The hot press was heated at ~1 °C/min from room temperature to 600 °C and then held at 600 °C for 360 min. The isothermal hold at 600 °C allowed the reaction between Zr and B to proceed without igniting an SHS reaction. After this hold, the hot press was heated at a rate of 10 °C/min to 1000 °C followed by an isothermal hold of 60 min Next, the hot press was heated at 10 °C/min to 1450 °C followed by another 60 min isothermal hold to allow for volatilization of any $B_2O_3$ that may have been present. The hot press was then heated at 5 °C/min to 1650 °C where it was held for 60 min based on a previous study that reported volatilization at this temperature.[5] After the isothermal hold at 1650 °C, the hot press was then backfilled with argon and heated at 50 °C/min to 2100 °C for densification. At 2100 °C, a pressure of 40 MPa was applied for 45 min. After 45 min, the furnace was cooled at 20 °C/min to room temperature. The load was released at ~1750 °C.

### 2.3. Hot pressed ceramics

XRD and SEM (S-4700, Hitachi, Tokyo, Japan) analyses were performed to characterize phase development and particle coarsening during reactive hot pressing. Powders heated to 600 °C, 1450 °C, 1650 °C, and 2100 °C were analyzed. For XRD, the full width at half maximum ($\beta$) was measured for each peak using a whole pattern fitting routine (JADE 5.026, Material Data Inc., Livermore, CA). Particle size and strain analysis were performed for the Zr–B powder mixtures heated to 600 °C using the Williamson–Hall method.[29] The slope of the Williamson–Hall plot is equal to the strain while the particle size is related to the $y$-axis intercept by Eq. (2):

$$y\text{-intercept} = \frac{0.9\lambda}{t} \quad (2)$$

where $\lambda$ = X-ray wavelength (1.5405 Å) $t$ = crystallite size (Å).

Because the peak widths for specimens heated to 1450 °C and 1650 °C were not sufficient for Williamson–Hall analysis, SEM images were analyzed to determine the crystallite size of the $ZrB_2$ at those temperatures. After hot pressing, the bulk density of the $ZrB_2$ billets was determined using the Archimedes' principle. The microstructures of polished, thermally etched specimens were examined using SEM. Grain size was determined from SEM images using image analysis software (ImageJ, National Institutes of Health, Bethesda, MD). Reported values were calculated from at least 125 individual grains. Phase analysis of hot pressed billets was performed using XRD. Additional chemical analysis was performed using ICP-MS to determine the oxygen content of RHP $ZrB_2$.[a]

Elastic constants were measured according to ASTM standard C1259-01 for impulse excitation on ~2 inch cylindrical discs (Grindosonic, J.W. Lemmens, St. Louis, MO). Four-point flexure strength was measured according to ASTM standard C1161–02a for type A bars (1.5 mm × 2 mm × 25 mm). A total of seven bars were fractured to determine the average strength and standard deviations.

## 3. Results and discussion

### 3.1. Reaction studies and powder characterization

Diffusion couples of Zr and B were prepared. Analysis of the cross-section of a couple heated to 1450 °C for 45 min (Fig. 1) revealed that a layer of $ZrB_2$ grew from the original Zr–B interface into the Zr metal. This conclusion is consistent with the previous reports that the particle size of reactively formed $ZrB_2$ was similar to the particle size of the starting Zr, which allowed the authors to infer that B diffused into Zr to form the final product.[23] From the current study and the results reported in the literature, it can be concluded that the size and shape of reactively formed $ZrB_2$ will be dictated by the size and shape of the Zr metal precursor particles. In the present study, attrition milling was used to reduce the Zr particle size prior to reaction.

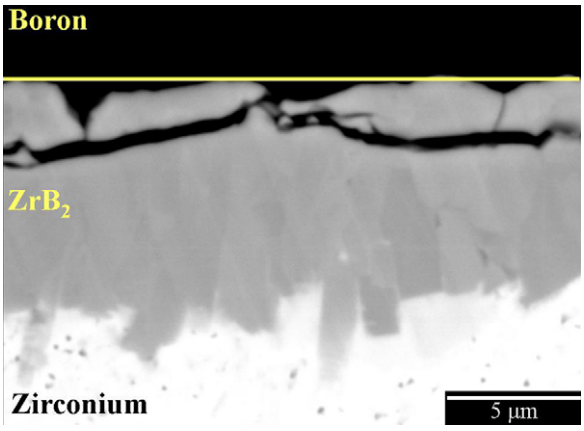


Fig. 1. Zr–B diffusion couple heated to 1450 °C for 45 min showing the growth of $ZrB_2$ from the original Zr–B interface into the Zr.

Attrition milling produces a high shear environment that promotes particle size reduction and intimate mixing. During the early stages of milling, the equiaxed starting Zr particles were deformed into platelet-like particles due to their ductility. Fig. 2 shows that after 60 min of milling, large Zr platelets (80–100 μm wide, ~10 μm thick) were formed. Based on literature reports, the elongation of the Zr particles probably occurred along the [1 $\bar{2}$ 0 1] direction with the (1 0 $\bar{1}$ 0) as the slip plane in α-zirconium, which has a hexagonal unit cell.[30,31] Increased milling times led to fracture of the Zr platelets into smaller particles, probably due to strain hardening induced by the deformation. XRD analysis of Zr powder milled for 240 min showed significant peak broadening compared to powder milled for 20 min (Fig. 3). The peak broadening observed for 240 min of milling is characteristic of nanosized crystallites (<200 nm) and/or strains greater than ~0.05%. Precise particle size and strain calculations were not possible for this powder using the Williamson–Hall approach since the number of distinct peaks was small. Instead, particle size was estimated using the Scherrer formula (Eq. (1)). From the broadening and position of (0 0 0 2) and (1 0 $\bar{1}$ 1) diffraction peaks, a Zr particle size of 15 nm was estimated, although this analysis may underestimate particle size since it does not account for non-uniform strain that may be induced during the particle size reduction process. Along with

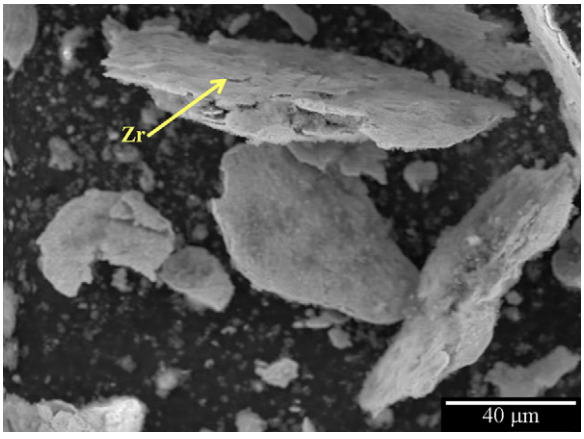


Fig. 2. Morphology of Zr powder particles after attrition milling for 60 min.

[a] Oxygen analysis performed by NSL Analytical Services, Cleveland, OH.

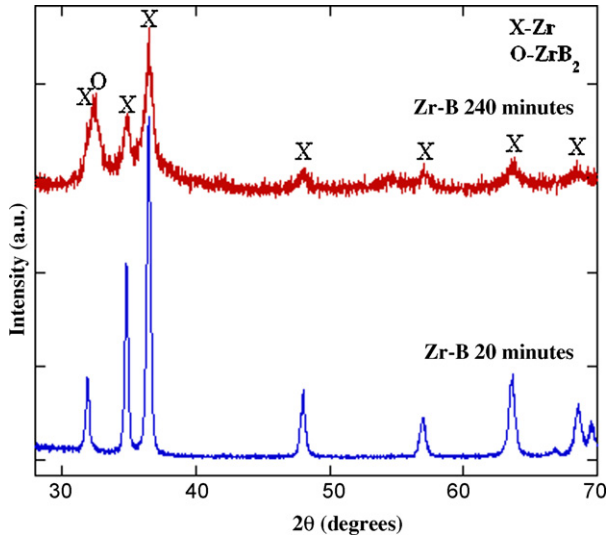


Fig. 3. XRD patterns of Zr–B mixtures milled for 20 and 240 min showing that the Zr peak width increased significantly and that a $ZrB_2$ (1 0 0) peak developed for longer milling times.

the particle size reduction, attrition milling also led to partial reaction of the precursors. Analysis of XRD patterns showed that for milling times of 120 min or more (240 min shown) a diffraction peak appeared that was consistent with the (1 0 0) peak for $ZrB_2$. The presence of only the (1 0 0) diffraction peak suggests that the formation of $ZrB_2$ may have only occurred on the surface of the deformed Zr particles and that the $ZrB_2$ may have been preferentially oriented. Based on the analysis of particle size, a milling time of 240 min was selected for processing of $ZrB_2$ because it provided sufficient particle size reduction and mixing necessary to ensure complete reaction at low temperatures.

Differential thermal analysis (DTA) of the Zr–B mixtures (Fig. 4) was used to characterize the reaction as a function of milling time. The analysis of the Zr–B powder mixtures milled for times ranging from 60 min to 240 min revealed broad exothermic peaks over temperatures ranging from below 500 °C to more than 1000 °C, suggesting the reaction occurred over a broad temperature range. As milling time increased, the exothermic reaction appeared to shift to slightly lower temperatures. Increased milling times resulted in an increase in surface area, which could result in a decrease in the reaction temperature due to more intimate mixing of the precursors.[32,33] After 120 min of milling the area under the exothermic curve appeared to decrease. The decrease in area suggests that the amount of heat generated by the reaction decreased, which would be expected since $ZrB_2$ was detected in powders that had milling times longer than about 120 min. Conversion of part of the Zr and B to $ZrB_2$ would reduce the amount of heat released during analysis since a portion of the specimen would have already reacted during milling. Partial reaction during milling should also reduce the adiabatic temperature and reaction rate,[32] which would inhibit ignition of an SHS reaction as desired for controlled reactive hot pressing. Accurate analysis of the onset temperatures, and the area under the exothermic curves, was not possible due to the broad exothermic peaks and non-level baseline observed for these materials.

Because nanoscale Zr particles were formed during milling, the reaction between Zr and B initiated below 600 °C. Based on XRD analysis (Fig. 5) of attrition milled powders, the reaction was complete after heating to 600 °C for 360 min since no residual Zr was detected. The XRD pattern for the mixture of Zr and B heated to 600 °C did reveal that a significant amount of $ZrO_2$ was present. Since $ZrO_2$ was not detected in the milled powder prior to heating, the formation of the oxide most likely occurred either during reaction or when the samples were exposed to air upon removal from the furnace. The latter seems likely since powders were observed to heat spontaneously when exposed to air upon removal from the furnace. Since oxidation is exothermic, heat should be evolved when $ZrB_2$ is converted to $ZrO_2$. Fortunately, $ZrO_2$ should not form by this mechanism during reactive

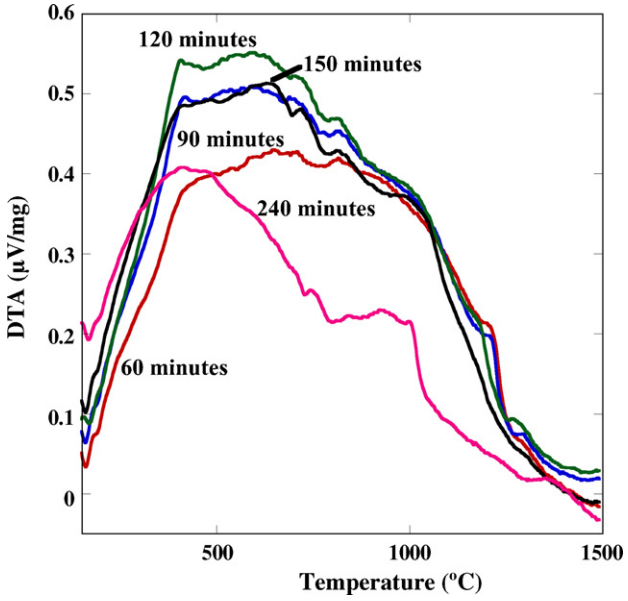


Fig. 4. DTA of Zr–B mixtures as a function of attrition milling time.

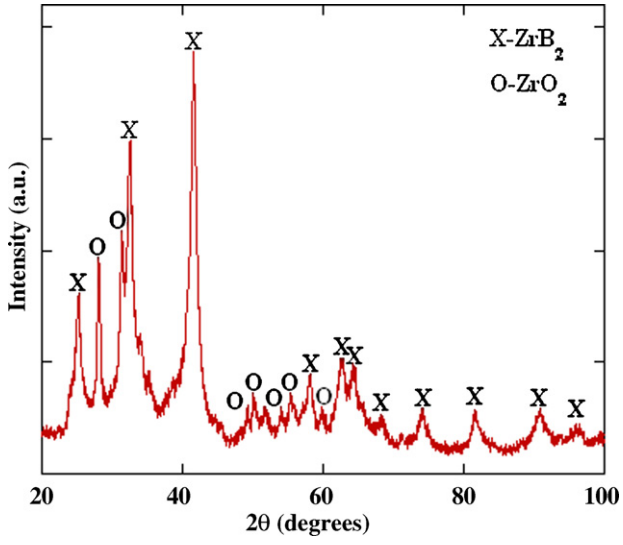


Fig. 5. XRD pattern of a Zr–B mixture heated to 600 °C for 360 min showing that $ZrO_2$ was present after exposure to air.

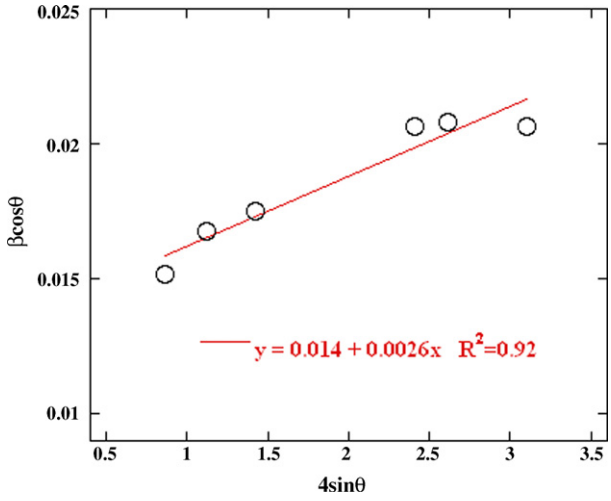


Fig. 6. A Williamson–Hall plot for a Zr–B mixture milled for 240 min and heated to 600 °C for 360 min.

hot pressing of $ZrB_2$ since reaction and densification are conducted in a single step without exposing the reacted material to air. Any $ZrO_2$ found in materials produced by the combined *in situ* reaction and densification process would be due to oxygen impurities in the starting materials.

Williamson–Hall analysis (Fig. 6) of the diffraction pattern for the Zr–B mixture that was milled for 240 min and then reacted at 600 °C for 360 min showed that the $ZrB_2$ had a crystallite size of ~10 nm and a compressive strain of ~0.26%. Analysis of SEM images of the Zr–B mixtures heat treated at 600 °C (Fig. 7a) confirmed that reactively formed $ZrB_2$ had a fine crystallite size (less than ~50 nm). Additional heat treatments to 1450 °C (Fig. 7b) and 1650 °C (Fig. 7c) led to significant coarsening of the $ZrB_2$ particles. At 1450 °C and 1650 °C, the average particle sizes increased to 0.6 μm and 1 μm, respectively. Measurement of the geometric density of specimens produced at 600 °C and 1650 °C showed a small increase in relative density from ~35% to ~40%. These results indicate that both coarsening and densification were possible at these moderate temperatures. The production of nanoscale particles by the low temperature reaction also allowed for the retention of sub-micron grains at temperatures as high as 1650 °C.

The grain coarsening that was observed between 600 °C and 1450 °C suggested that the nanoscale $ZrB_2$ particles had a large driving force for sintering. Particle coarsening of nanosized diboride powders has been reported below 1700 °C.[34] However, coarsening of micron-sized non-reactive $ZrB_2$ particles generally occurs above ~1650 °C due to the presence of surface oxides that promote transport processes that lead to coarsening in preference to densification.[35] The increased driving force for sintering most likely exists for two reasons: the $ZrB_2$ particle size and high defect concentrations. A larger concentration of defects is expected in the $ZrB_2$ formed *in situ* compared to commercial powders due to the extensive attrition milling used to reduce the Zr particle size, which would be expected to induce lattice defects into the Zr. The low temperature reaction used to form the $ZrB_2$ may not have provided sufficient thermal energy for the relaxation of defects through normal mechanisms. A large concentration of defects has been linked to enhanced densification of diboride materials.[27] Thus, the coarsening and densification observed between 600 °C and 1450 °C may be enhanced by a combination of particle size and the presence of defects.

### 3.2. Densification and microstructure

Despite the increase in density and the significant coarsening observed at modest temperatures (e.g., 1650 °C), an ultimate temperature of 2100 °C was required to achieve full density (>99%) for $ZrB_2$ produced by reactive hot pressing. Analysis of polished cross-sections confirmed that RHP $ZrB_2$ (Fig. 8) produced at 2100 °C had minimal amounts of porosity. For

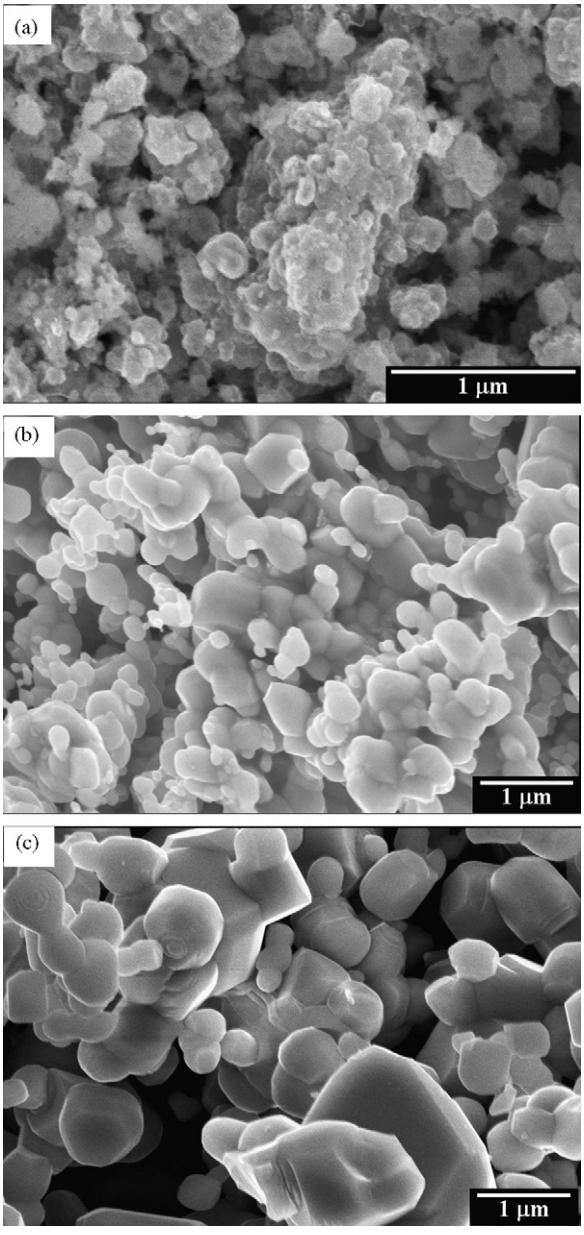


Fig. 7. SEM micrographs of $ZrB_2$ formed from Zr–B powder mixtures milled for 240 min after heating to (a) 600 °C for 360 min, (b) 1450 °C for 60 min, and (c) 1650 °C for 60 min (*note*: magnification changes with heat treatment temperature).

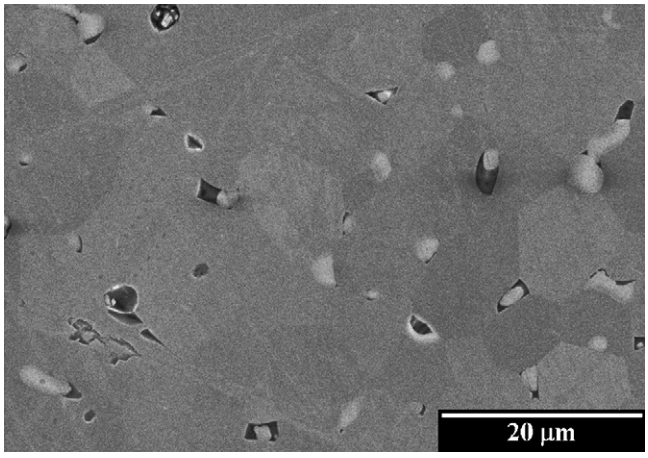


Fig. 8. A polished cross-section of $ZrB_2$ produced by reactive hot pressing at 2100 °C.

comparison, dense $ZrB_2$ can be produced by conventional hot pressing of commercial powders at least 200 °C below the temperature used for RHP. The higher temperature required for densification of RHP $ZrB_2$ was attributed to the significant coarsening of the powder that occurred during the isothermal heat treatments.[5] The increase in average particle size that occurred at 1450 °C and 1650 °C would have led to a significant decrease in the surface area and, perhaps, in the concentration of any defects that resulted from attrition milling of the precursors. As a result, the driving force for densification would also be expected to decrease at these temperatures. Reduction in the driving force for densification prior to the application of pressure could explain the need for the processing temperature of 2100 °C. Thus, the particle coarsening that occurred after reaction most likely diminished the driving for sintering, which was expected to be enhanced for the nanoscale $ZrB_2$ formed by the *in situ* reaction/densification process.

Qualitative phase analysis of RHP $ZrB_2$ using XRD (Fig. 9) showed that $ZrB_2$ and trace amounts of $ZrO_2$ were the only

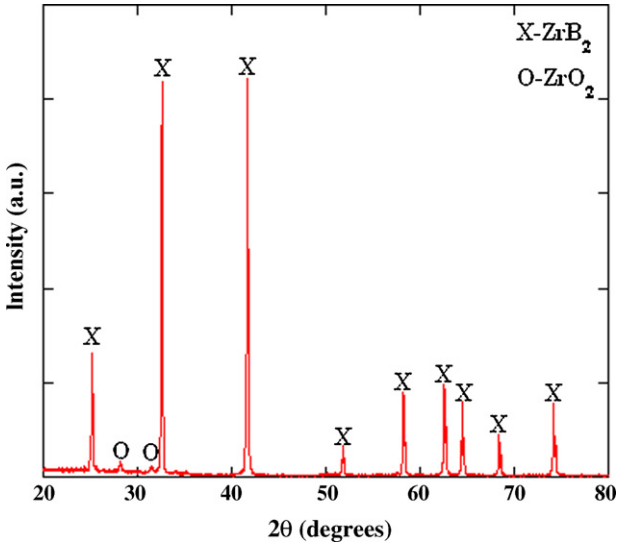


Fig. 9. XRD of RHP $ZrB_2$ showing that only two crystalline phase are present; $ZrB_2$ and $ZrO_2$.

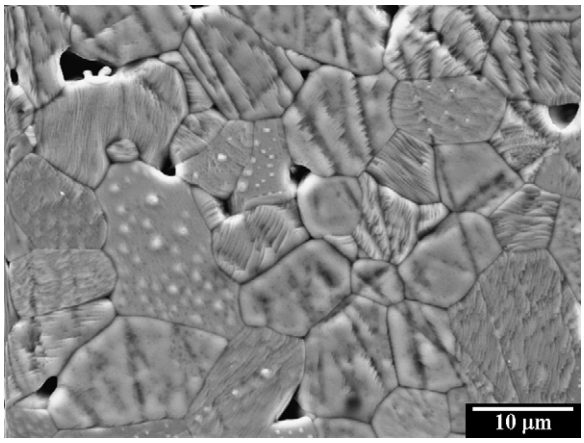


Fig. 10. SEM micrograph of thermally etched RHP $ZrB_2$.

crystalline phases present after hot pressing. Oxygen impurities are known to promote coarsening of $ZrB_2$ and other non-oxide ceramics at temperature below which densification is possible, which reduces the driving force for densification. Quantitative chemical analysis of the oxygen content showed that on average 2.4 wt.% oxygen was present in RHP samples, which is a 20% increase from the 2 wt.% found in non-reactive $ZrB_2$.[35] The higher level of oxygen in the RHP material may be a consequence of the higher surface area of the nanoscale particles produced by the reactive process; specifically, the high surface area Zr produced by attrition milling likely had a surface oxide layer that led to the incorporation of $ZrO_2$ into the final $ZrB_2$. In previous studies, it was shown that reactive additives such as tungsten carbide and boron carbide reacted with and removed the $ZrO_2$,[15,35] which enabled densification without the application of pressure. Thus, the addition of reactive additives to the Zr–B mixture may reduce the amount of oxygen in the final material and enable densification at lower temperatures.

The grain size of RHP $ZrB_2$ was significantly larger than the grain size of $ZrB_2$ produced by conventional hot pressing. For RHP materials, the average grain size was $12.0 \pm 6.0\,\mu m$ (Fig. 10), which is a 100% increase when compared to non-reactive $ZrB_2$ produced by conventional hot pressing that had a grain size of $6.0 \pm 3.0\,\mu m$.[5] The increase in grain was a result of the higher temperature required for densification of the reactively formed $ZrB_2$ compared to the conventional process. Densification at 2100 °C is thought to be accomplished through plastic flow and volume diffusion mechanisms that can lead to enlarged grains in diboride materials.[16] In addition, the higher oxygen content of the reactively formed material may have resulted in coarsening at modest temperatures (e.g., 1650 °C or below). Thus, minimizing the oxygen content of the reactive mixture may reduce the hot pressing temperature required for densification and result in a finer grain sizes.

### 3.3. Mechanical properties

The elastic modulus of RHP $ZrB_2$ was 510 GPa, which is similar to values reported for conventionally hot pressed $ZrB_2$ (490 GPa). The moduli should be similar since modulus is an

intrinsic material property that is not significantly affected by grain size or other processing variables.

The flexure strength of $ZrB_2$ produced by RHP was $434 \pm 65$ MPa. The strength of RHP $ZrB_2$ was lower than non-reactive $ZrB_2$, which had an average strength of 560 MPa.[5] The lower strength of the RHP $ZrB_2$ was presumably due to its increased grain size, which was a result of the increased hot pressing temperature required for densification. A significant increase in the strength of RHP $ZrB_2$ may be possible if the hot pressing temperature can be reduced, which would result in a decreased grain size.

## 4. Conclusions

Nanoscale $ZrB_2$ particles were formed using a controlled reaction between elemental Zr and B. The Zr and B precursors, with average crystallite sizes of ~10 nm, were produced by attrition milling and then reacted to produce nanosized $ZrB_2$ crystallites. Because of the fine precursor particle size and the intimate mixing, the reaction of Zr and B to $ZrB_2$ went to completion at 600 °C. The nano-crystalline $ZrB_2$ exhibited significant coarsening and densification between 600 °C and 1450 °C, which was result of the fine particle size and the, possibly, a high defect concentration. Significant particle coarsening below 1650 °C decreased the sinterability of the $ZrB_2$. As a result, processing temperatures of 2100 °C were required to achieve full density. Consolidation of RHP $ZrB_2$ at 2100 °C resulted in large grains (~12 μm), which led to a lower flexure strength (430 MPa) compared to $ZrB_2$ produced by conventional hot pressing in previous studies.

## Acknowledgement

This work was funded by the Air Force Office of Scientific Research on contract number FA9550-06-1-0125.

## References

1. Kumashiro, Y., Survey of refratory metalloids: transition metal carbides, nitrides, and diborides. In *Electric Refractory Materials*, ed. Y. Kumashiro. Marcel Dekker, New York, 2000, pp. 7–17.
2. Vajeeston, P., Ravindran, P., Ravi, C. and Asokamani, R., Electron structure, bonding, and ground-state properties of AlB2-type transition metal diborides. *Phys. Rev. B*, 2001, **63**, 045115/1-045115/12.
3. Mulokozi, A. M., Electron transfer and bonding in the transition metal diborides: the heats of formation of the metal diborides derived from a theoretical bonding model. *J. Less-Common Met.*, 1979, **64**, 145–153.
4. Fahrenholtz, W. G., Hilmas, G. E., Talmy, I. G. and Zaykoski, J. A., Refractory diborides of zirconium and hafnium. *J. Am. Ceram. Soc.*, 2007, **90**, 1347–1364.
5. Chamberlain, A. L., Fahrenholtz, W. G., Hilmas, G. E. and Ellerby, D. T., High strength zirconium diboride-based ceramics. *J. Am. Ceram. Soc.*, 2004, **87**, 1170–1172.
6. Cutler, R. A., Engineering properties of borides. In *Ceramics and Glasses, Engineered Materials Handbook*, *vol. 4*, ed. S. J. Schneider. ASM International, Materials Park, OH, 1992, pp. 787–803.
7. Zimmermann, J. W., Hilmas, G. E., Fahrenholtz, G. E., Dinwiddie, R., Porter, W. and Wang, H., Thermophysical properties of $ZrB_2$-based ceramics. *J. Am. Ceram. Soc.*, 2008, **91**, 1405–1411.
8. Upadhya, K., Yang, K. and Hoffman, W., Materials for ultrahigh temperature structural applications. *Am. Ceram. Soc. Bull.*, 1997, **76**, 51–56.
9. Kaufmann, L. and Nesor, H., *Stability Characterization of Refractory Materials under High Velocity Atmospheric Flight Conditions, Part I, vol. I, Summary*. Technical Report No. AMFL-TR-69-84, Air Force Materials Laboratory, Wright-Patterson Air Base, OH, 1970.
10. Bull, J. and Rasky, D., Stability characterization of diboride composites under high velocity atmospheric flight conditions. *Presented at the 24th International SAMPE Conference*, T1092-T1106 October 20–22, 1992.
11. Monteverde, F., Bellosi, A., Guicciardi, S. and Processing, Properties of zirconium diboride-based composites. *J. Eur. Ceram. Soc.*, 2002, **22**, 279–288.
12. Bellosi, A., Monteverde, F., Fabriche, D. and Melandri, C., Microstructure and properties of $ZrB_2$-based ceramics. *J. Mater. Proc. Manuf. Sci.*, 2001, **9**, 156–170.
13. Monteverde, F., Guicciadri, S. and Bellosi, A., Advances in microstructure and mechanical properties of zirconium diboride based ceramics. *Mater. Sci. Eng.*, 2003, **A346**, 310–319.
14. Opila, E., Levine, S. and Lorincz, J., Oxidation of $ZrB_2$- and $HfB_2$-based ultra-high temperature ceramics: effect of Ta additions. *J. Mater. Sci.*, 2004, **38**, 5969–5977.
15. Zhang, S. C., Hilmas, G. E. and Fahrenholtz, W. G., Pressureless densification of zirconium diboride with boron carbide additions. *J. Am. Ceram. Soc.*, 2006, **89**, 1544–1550.
16. Telle, R., Sigl, L. S. and Takagi, K., Boride-based hard materials. In *Handbook of Ceramic Hard Materials*, *vol. 2*, ed. R. Riedel. Wiley-VCH, Weinheim, 2000, pp. 802–945.
17. Radev, D. D. and Marinov, M., Properties of Titanium and zirconium diboride obtained by self-propagated high temperature synthesis. *J. Alloys Compd.*, 1996, **244**, 48–51.
18. Mishra, S. K., Das, S., Das, S. K. and Ramachandrarao, P., Sintering studies on ultrafine $ZrB_2$ powder produced by a self-propagating high-temperature synthesis process. *J. Mater. Res.*, 2000, **15**, 2499–2504.
19. Chiang, Y.-M., Haggerty, J. S., Messner, R. P. and Demetry, C., Reaction-based processing methods for ceramic–matrix composite. *Am. Ceram. Soc. Bull.*, 1989, **68**, 420–428.
20. Subrahmanyam, J., Vijaykumar, M. and Ranganath, S., Thermochemistry of self-propagating high temperature synthesis of titanium diboride composites. *Met. Mater. Process.*, 1989, **1**, 105–112.
21. Zhang, G.-J., Yang, J.-F., Ando, M. and Ohji, T., Reactive hot pressing of alumina-silicon carbide nanocomposites. *J. Am. Ceram. Soc.*, 2004, **57**, 299–301.
22. Fahrenholtz, W. G., Ellerby, D. T. and Loehman, R. E., $Al_2O_3$–Ni composites with high strength and fracture toughness. *J. Am. Ceram. Soc.*, 2000, **83**, 1279–1280.
23. Zhang, G.-J., Deng, Z.-Y., Kondo, N., Yang, J.-F. and Ohji, T., Reactive hot pressing of $ZrB_2$–SiC composites. *J. Am. Ceram. Soc.*, 2000, **83**, 2330–2332.
24. Monteverde, F., Progress in the fabrication of ultra-high-temperature ceramics: "in-situ" synthesis, microstructure, and properties of a reactive hot-pressed $HfB_2$–SiC composites. *Comp. Sci. Technol.*, 2005, **65**, 1869–1879.
25. Chamberlain, A. L., Fahrenholtz, W. G. and Hilmas, G. E., Low temperature densification of zirconium diboride ceramics by reactive hot pressing. *J. Am. Ceram. Soc.*, 2006, **89**, 3638–3645.
26. Gasch, M., Ellerby, D., Irby, E., Beckman, S., Gusman, M. and Johnson, S., Processing, properties, and arc jet oxidation of hafnium diboride/silicon carbide ultra high temperature ceramics. *J. Mater. Sci.*, 2004, **39**, 5925–5937.
27. Kisliy, P. S., Kuzenkova, M. A. and Zaveruha, O. V., The effect of the particle size of powders on the sintering kinetics of titanium diboride. *Phys. Sint.*, 1972, **4**, 107–118.
28. Jenkins, R. and Synder, R. L., Diffraction theory. *Introduction to X-ray Powder Diffractometry*. John Wiley & Sons, New York, 1996, p. 47–97.
29. Williamson, G. K. and Hall, W. H., X-ray line broadening from filed aluminum and tungsten. *Acta Met.*, 1953, **1**, 22–31.

30. Askeland, D. R. and Phule, P. P., Imperfection in the atomic and ionic arrangements. *The Science and Engineering of Materials* (*4th edition*). Brookes/Cole-Thomson Learning, Southbank, Victoria, 2003, p. 129–217.
31. Sokurskii, I. N. and Protsenko, L. N., Deformation systems of α-zirconium. *Atomic Energy*, 1958, **4**, 579–582.
32. Fahrenholtz, W. G., Reactive hot pressing of $Al_2O_3$–Ni composites. *J. Mater. Sci.*, 2003, **38**, 3073–3080.
33. Mossino, P., Some aspects in self-propagating high temperature synthesis. *Ceram. Int.*, 2004, **30**, 311–332.
34. Baik, S. and Becher, P. F., Effect of oxygen contamination on densification of $TiB_2$. *J. Am. Ceram. Soc.*, 1987, **70**, 527–530.
35. Chamberlain, A. L., Fahrenholtz, W. G. and Hilmas, G. E., Pressureless sintering of zirconium diboride. *J. Am. Ceram. Soc.*, 2006, **89**, 450–456.